

A | Appendix

Here, we present supporting (additional) information of our research works.

A.1 Supporting Information of Chapter 3

TABLE A.1: The Co-atom binding energy ($E_b(\text{Co})$), average C-Co bond length $d_{av}(\text{C-Co})$ and optimized site for particular initial site.

Site	$E_b(\text{Co})$ (eV)	$d_{av}(\text{C-Co})$ (eV)	Final Site
T1	-3.02	1.90	T1
T2	-3.36	2.04	H4
T3	-2.80	2.10	T3
T4	-3.17	2.07	H4
H1	-3.23	2.17	H1
H2	-3.19	2.17	H2
H3	-3.19	2.17	H3
H4	-3.37	2.04	H4
B1	-3.37	2.04	H4
B2	-3.37	2.04	H4
B3	-3.37	2.04	H4
B4	-3.14	2.12	H2
B5	-2.80	2.10	T3
B6	-2.84	1.96	B6

A.2 Supporting Information of Chapter 4

In Table A.2, we provided the binding energy of M-atoms over AlN at Al-d site. We also provided exact values of interaction energies of reactants on considered M@AlN. In Table A.3, we provided computed activation energies and reaction energy of WGS reaction via formate mechanism over M@AlN. In Table A.4, we provided computed activation energies and reaction energy of WGS reaction via OH-assistive mechanism over M@AlN. The complete reaction profile of WGS reaction via formate mechanism on Ni/Pd/Pt/Cu/Ag@AlN are depicted in Fig.A.1 to Fig.A.5, respectively. The complete reaction profile of WGS reaction via OH-assistive mechanism on Ni/Pd/Pt/Ag@AlN are depicted in Fig.A.6 to Fig.A.9, respectively.

TABLE A.2: The binding energy (E_b) of M@AlN and adsorption/co-adsorption (E_{ads}) energies of reactants over M@AlN.

System	E_b (eV)	$E_{ads}(\text{CO})$ (eV)	$E_{ads}(\text{OH})$ (eV)	$E_{ads}(\text{CO}+\text{OH})$ (eV)	$E_{ads}(\text{H}_2\text{O})$ (eV)	$E_{ads}(\text{CO}+\text{H}_2\text{O})$ (eV)
Ni@AlN	-6.89	-1.13	-3.34	-4.61	-3.94	-5.29
Pd@AlN	-5.87	-2.19	-3.98	-5.05	-4.17	-6.02
Pt@AlN	-6.56	-1.57	-3.89	-5.39	-4.02	-5.61
Cu@AlN	-4.92	-1.04	-2.65	-3.77	-3.66	-4.87
Ag@AlN	-4.64	-0.87	-3.01	-3.93	-3.71	-4.74
Au@AlN	-4.37	-0.9	-2.73	-3.68	-3.59	-4.44

TABLE A.3: The computed reaction barriers and reaction energy of WGS reaction via formate mechanism over M@AlN.

System	E_a (first barrier) (eV)	E_a (second barrier) (eV)	E_R (eV)
Ni@AlN	1.16	0.37	0.97
Pd@AlN	1.05	0.45	1.26
Pt@AlN	0.96	0.31	1.15
Cu@AlN	0.68	0.3	1.24
Ag@AlN	0.73	0.29	1.13
Au@AlN	0.51	0.21	1.19

TABLE A.4: The computed reaction barriers and reaction energy of WGS reaction via OH-assistive mechanism over M@AlN.

System	E_a (first barrier) (eV)	E_a (second barrier) (eV)	E_R (eV)
Ni@AlN	0.72	0.18	0.84
Pd@AlN	0.81	0.29	0.87
Pt@AlN	1.04	0.56	0.73
Cu@AlN	0.21	0.11	1.18
Ag@AlN	0.56	0.21	0.92
Au@AlN	0.14	0.08	1.25

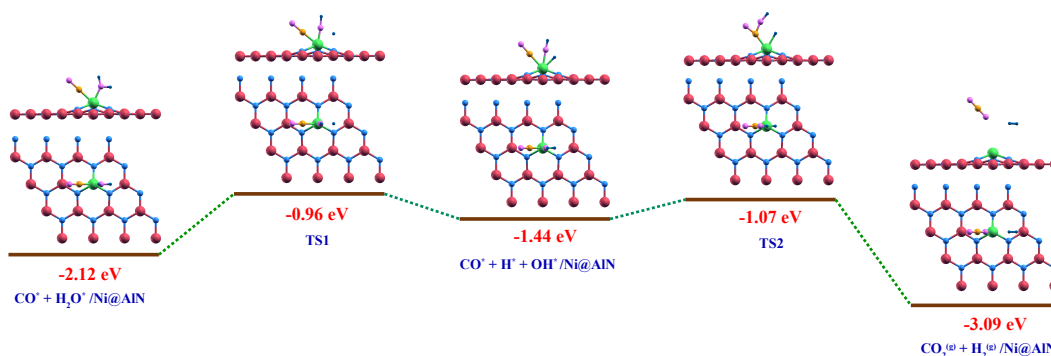


FIGURE A.1: The complete reaction profile and optimized geometric configurations of various states for WGS reaction via formate mechanism on Ni@AlN.

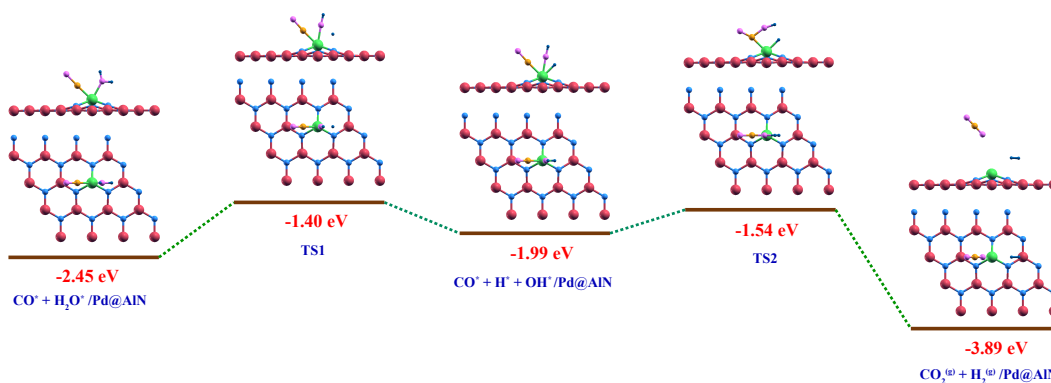


FIGURE A.2: The complete reaction profile and optimized geometric configurations of various states for WGS reaction via formate mechanism on Pd@AlN.

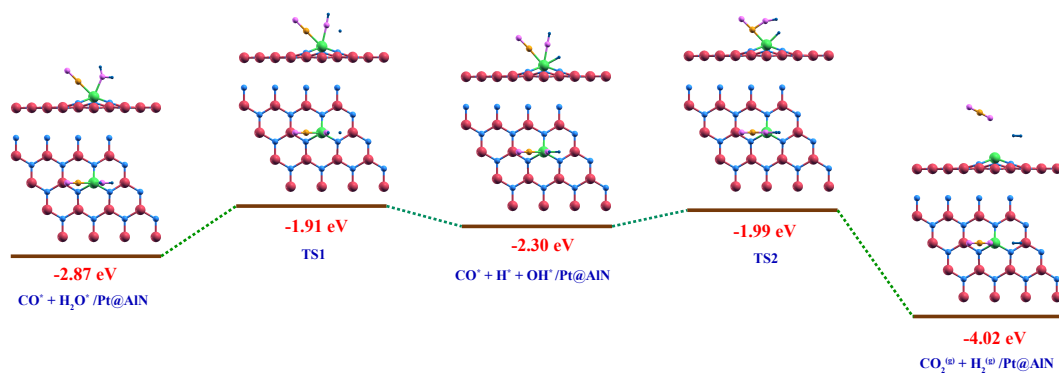


FIGURE A.3: The complete reaction profile and optimized geometric configurations of various states for WGS reaction via formate mechanism on Pt@AlN.

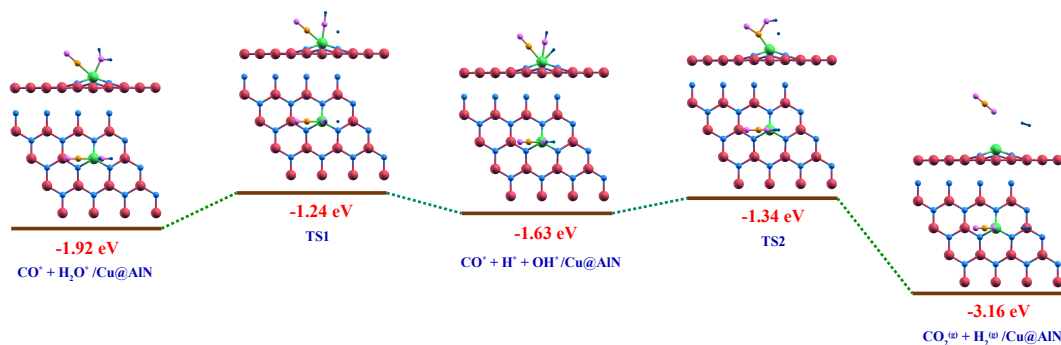


FIGURE A.4: The complete reaction profile and optimized geometric configurations of various states for WGS reaction via formate mechanism on Cu@AlN.

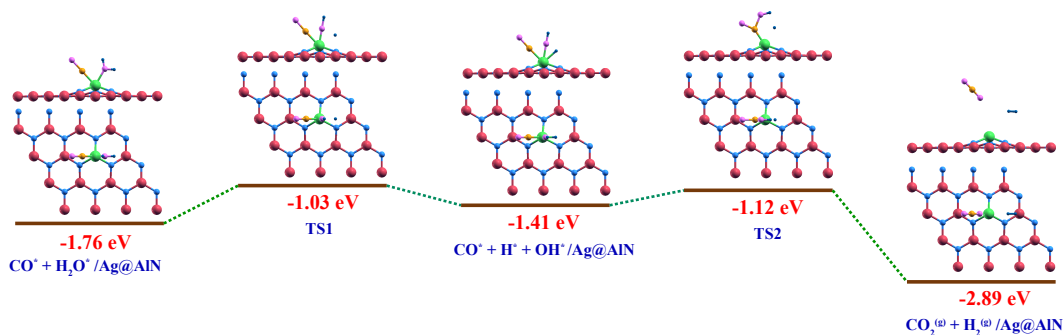


FIGURE A.5: The complete reaction profile and optimized geometric configurations of various states for WGS reaction via formate mechanism on Ag@AlN.

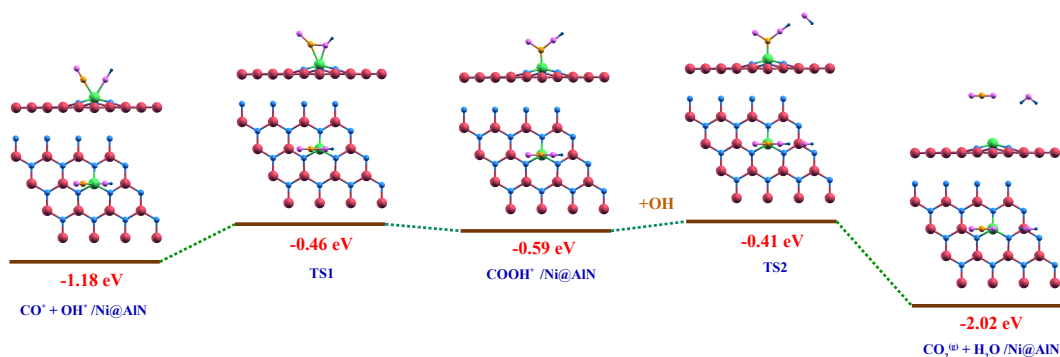


FIGURE A.6: The complete reaction profile and optimized geometric configurations of various states for WGS reaction via OH-assistive mechanism on Ni@AlN.

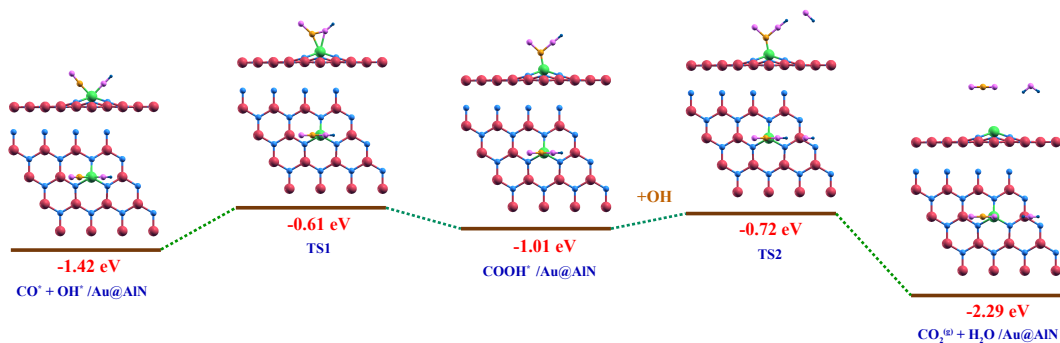


FIGURE A.7: The complete reaction profile and optimized geometric configurations of various states for WGS reaction via OH-assistive mechanism on Pd@AlN.

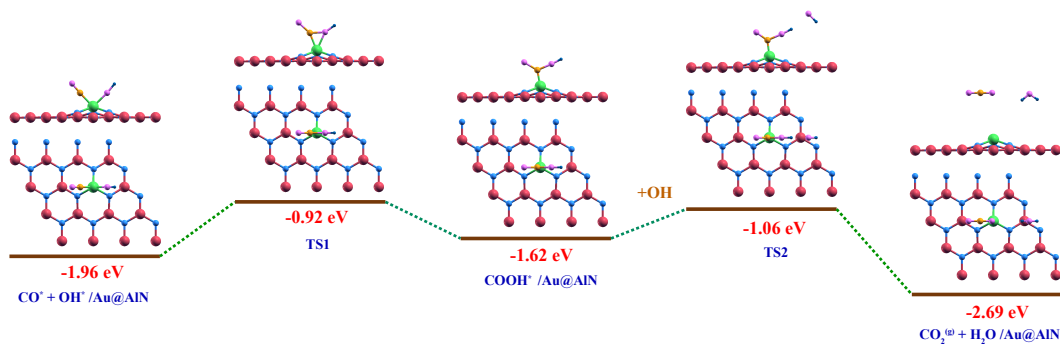


FIGURE A.8: The complete reaction profile and optimized geometric configurations of various states for WGS reaction via OH-assistive mechanism on Pt@AlN.

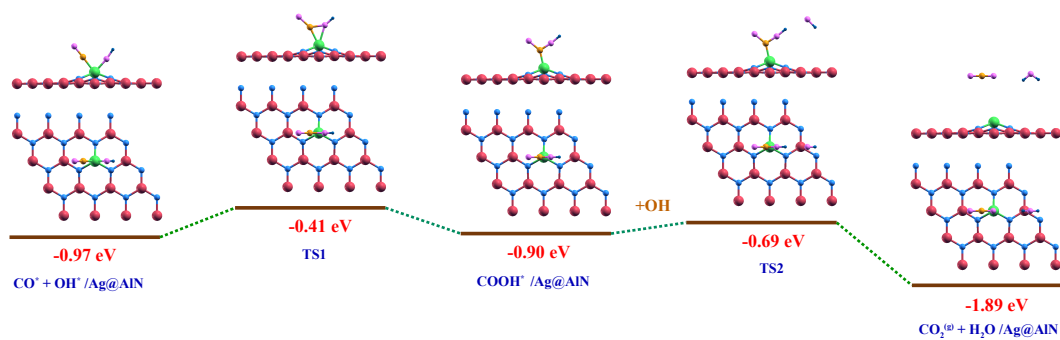


FIGURE A.9: The complete reaction profile and optimized geometric configurations of various states for WGS reaction via OH-assistive mechanism on Ag@AlN.